

## Journal Pre-proof

Combining high throughput ASD screening with the rDCS to streamline development of poorly soluble drugs

Malte Bøgh Senniksen , Nicole Wyttenbach , Susanne Page , Jennifer Dressman

PII: S0928-0987(25)00129-0  
DOI: <https://doi.org/10.1016/j.ejps.2025.107130>  
Reference: PHASCI 107130



To appear in: *European Journal of Pharmaceutical Sciences*

Received date: 10 March 2025  
Revised date: 12 May 2025  
Accepted date: 15 May 2025

Please cite this article as: Malte Bøgh Senniksen , Nicole Wyttenbach , Susanne Page , Jennifer Dressman , Combining high throughput ASD screening with the rDCS to streamline development of poorly soluble drugs, *European Journal of Pharmaceutical Sciences* (2025), doi: <https://doi.org/10.1016/j.ejps.2025.107130>

This is a PDF file of an article that has undergone enhancements after acceptance, such as the addition of a cover page and metadata, and formatting for readability, but it is not yet the definitive version of record. This version will undergo additional copyediting, typesetting and review before it is published in its final form, but we are providing this version to give early visibility of the article. Please note that, during the production process, errors may be discovered which could affect the content, and all legal disclaimers that apply to the journal pertain.

© 2025 Published by Elsevier B.V.  
This is an open access article under the CC BY-NC-ND license (<http://creativecommons.org/licenses/by-nc-nd/4.0/>)

# Combining high throughput ASD screening with the rDCS to streamline development of poorly soluble drugs

Malte Bøgh Senniksen<sup>1,2</sup>, Nicole Wyttenbach<sup>3</sup>, Susanne Page<sup>2</sup>, and Jennifer Dressman<sup>1,\*</sup>

<sup>1</sup>Fraunhofer Institute for Translational Medicine and Pharmacology, Theodor-Stern-Kai 7, 60596 Frankfurt am Main, Germany

<sup>2</sup>Pharmaceutical R&D, F. Hoffmann-La Roche Ltd., Grenzacherstrasse 124, 4070 Basel, Switzerland

<sup>3</sup>Pharmaceutical Research & Early Development, Roche Innovation Center Basel, F. Hoffmann-La Roche Ltd., Grenzacherstrasse 124, 4070 Basel, Switzerland

\*Corresponding author e-mail address: [jdressman@em.uni-frankfurt.de](mailto:jdressman@em.uni-frankfurt.de) (J. Dressman)

## Abstract

Poor aqueous solubility and slow dissolution rate of active pharmaceutical ingredients (APIs) are often encountered challenges during oral drug development, leading to variable and insufficient bioavailability. To overcome these challenges, a so-called “enabling” formulation strategy is often pursued. Among these, amorphous solid dispersions (ASDs) are established as an effective means of improving drug absorption. However, evaluating the outcome of *in vitro* ASD screening approaches and relating this to the expected bioavailability increase can be difficult if not done systematically. Here we show, for the first time, how the combination of a high throughput ASD screening method with the refined Developability Classification System (rDCS) can streamline the formulation of poorly soluble APIs as ASDs. Using the Screening of Polymers for Amorphous Drug Stabilization (SPADS) approach to rapidly prepare ASD films, the improvement in dissolution performance of three APIs (befetupitant, celecoxib and itraconazole) was investigated with eight polymeric carriers. The results showed that the concentration of dissolved API was highly dependent on both the carrier and the drug load. For the APIs studied, Eudragit E, HPMC 100LV and Soluplus showed especially advantageous effects as carriers. Translating these results into the rDCS framework allowed for the visualization of the left-shift (more favorable for absorption) in classification. Several ASD films were classified as rDCS class I, showing a major improvement from the initial IIb classification of the pure API. This novel approach could be expanded to include a diverse set of screening methods for enabling formulation strategies, where the rDCS can allow for a direct comparison and support formulation selection.

Key words: Amorphous Solid Dispersion, Supersaturation, Dissolution, Oral absorption, High-throughput screening, Refined Developability Classification System (rDCS).

## Introduction

Introduced in 2010, the developability classification system (DCS) is recognized as a powerful tool during the early stages of drug development<sup>1</sup>. Depending on its biopharmaceutical profile, an active pharmaceutical ingredient (API) can be classified in one of four classes, with class II being further divided into IIa and IIb for APIs with dissolution rate limited and solubility limited absorption, respectively<sup>1</sup>. Since its introduction, the DCS has been further evolved into the refined developability classification system (rDCS), introducing *inter alia* a decision tree that is based on both standard and customized investigations. To address the fact that during preclinical development, the dose of an API is rarely already established, the rDCS encourages the use of a wide

potential dose range of 5, 50 and 500 mg<sup>2</sup>. Recently, the rDCS has received attention related to drugs which show supersaturation and precipitation effects<sup>3</sup> as well as to guide the design of oral formulations<sup>4</sup>.

For APIs with a dose classified as rDCS class IIb or IV, where solubility-limited absorption is anticipated, an enabling formulation is frequently sought to ensure sufficient *in vivo* exposure. Amorphous solid dispersions (ASDs) represent one such enabling formulation. The ASD approach aims to increase bioavailability by harnessing the high energy state of the amorphous API to achieve not only a faster dissolution rate but also supersaturation in the gastrointestinal tract<sup>5, 6</sup>. Ideally, an ASD is a molecular dispersion of the API within an amorphous carrier. The carrier, typically a hydrophilic polymer, impedes crystallization of the API in the solid state and can also serve to stabilize supersaturated solutions of the API upon dissolution<sup>6-8</sup>. For a detailed review of the mechanisms behind the bioavailability enhancement of ASDs the reader is referred to the comprehensive publication by Schittny *et al*<sup>9</sup>. For information regarding the manufacturing strategies available for ASDs the reader is referred to the thorough review of Bhujbal *et al*<sup>10</sup>.

Different approaches exist to screen potential ASD candidates for bioavailability enhancement and stability such as *in silico* methods<sup>11-13</sup> and melt-based screening methods<sup>14-16</sup>. To efficiently screen a range of ASD candidates with different carriers and drug loads for their ability to improve bioavailability, a film casting approach is often utilized, such as the Screening of Polymers for Amorphous Drug Stabilization (SPADS) workflow<sup>17</sup>. By utilizing 96-well microtiter plates to conduct film casting and dissolution testing, a wide range of samples can be investigated concurrently, with a small consumption of API. In the present study, three poorly water-soluble drugs (befetupitant, celecoxib and itraconazole) and eight different polymers were investigated. The polymers were chosen to reflect the variety of the carriers used in marketed ASD products as well as including polymers that are more novel for this purpose. Together, the polymers represent a wide range of functional moieties, hydrophilicity, glass transition temperatures and molecular weights.

This study sets out to combine the SPADS dissolution assay with rDCS classification. The proposed workflow i) classifies the APIs according to rDCS to identify the need for solubility improvement, ii) presents a detailed approach to dissolution screening of ASD films and iii) utilizes the rDCS to visualize the outcome of the screening approach. By combining these two approaches, the most suitable ASD strategy for a given poorly soluble drug can be identified, thus guiding decision-making during the early stages of formulation development.

## Materials

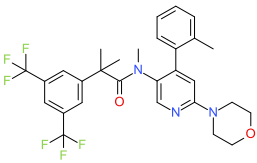
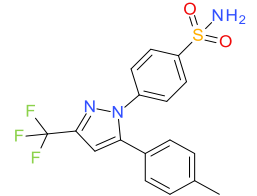
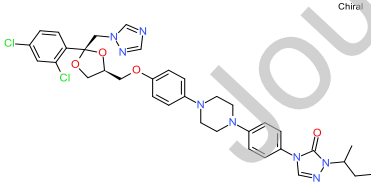
Crystalline befetupitant was provided by F. Hoffmann - La Roche Ltd (Basel, CH). Crystalline celecoxib was purchased from AA Blocks LLC (San Diego, CA, USA). Crystalline itraconazole was purchased from Chemieliva Pharmaceutical CO., Ltd (Chongqing, PRC) (Table 1.). Polyvinylpyrrolidone (PVP) K25, vinylpyrrolidone-vinyl acetate copolymer (PVP VA64) and Soluplus were kindly donated by BASF (Ludwigshafen, DE), Eudragit® E PO and L100 were purchased from Evonik (Essen, DE), AQOAT® Hypromellose Acetate Succinate-MMP (HPMCAS-MMP) was kindly donated by Shin-Etsu (Wiesbaden, DE), AFFINISOL™ Hypromellose (HPMC) 100LV kindly donated by Dupont de Nemours (Luzern, CH), Cellulose Acetate Phthalate (CAP) was purchased from Sigma-Aldrich (Steinheim, DE) (Table 2.). NaH<sub>2</sub>PO<sub>4</sub>, NaCl, NaOH and HCl were purchased from Merck KgaA (Darmstadt, DE). 3F Biorelevant powder was purchased from Biorelevant.com LTD (London, UK), and used to prepare fasted state simulated intestinal fluid (FaSSIF-V1). The solvents and diluent used for ultra performance liquid chromatography™ (UPLC) analysis were of an appropriate grade. Acetonitrile, formic acid and N-methyl-2-pyrrolidone (NMP) were purchased from VWR International (Rosny-sous-Bois cedex, FR).

## Methods

The selected APIs are summarized in Table 1. They were chosen to represent a typical range of molecular weights within the small molecule API paradigm and to possess different functional moieties. Preliminary tests revealed that the APIs exhibit differences in aqueous solubility (although all would be classified as poorly soluble according to all current classification systems) and degrees of glass forming ability, indicating that these APIs may be candidates for formulation as ASDs. Befetupitant is a discontinued development compound from F. Hoffmann - La Roche Ltd, for which no therapeutic dose has been defined, and could therefore be used in the rDCS framework as a true example of a development compound. For the two other APIs, literature examples already exist for the development of enabling formulations such as ASDs of celecoxib<sup>18-21</sup> and itraconazole<sup>22-25</sup>.

Table 1.

Selected APIs and their properties

API	M <sub>w</sub> [g mol <sup>-1</sup> ]	Log P <sup>a</sup>	pKa	T <sub>m</sub> [°C] <sup>b</sup>	T <sub>g</sub> [°C] <sup>b</sup>
 Befetupitant	565.6	5.8	3.7 <sup>c</sup> (basic)	129.2 ± 0.2	54.0 ± 0.4
 Celecoxib	381.4	4.0	11.1 <sup>26</sup> (acidic)	161.5 ± 0.1	56.8 ± 0.1
 Itraconazole	705.6	5.5	3.7 <sup>27</sup> (basic)	166.7 ± 0.2	58.5 ± 0.3

<sup>a</sup>Calculated according to ALogPS 2.1<sup>28</sup>

<sup>b</sup>Data generated in this study

<sup>c</sup>Data on file, Roche

T<sub>m</sub> values were taken as the average onset temperature of the melting endotherm for three samples

T<sub>g</sub> values were taken as the average midpoint temperature of glass transition upon reheating after 20 °C min<sup>-1</sup> cooling for three samples

To represent a broad variety of carriers, eight different polymeric carriers were chosen. These were selected to reflect the variety of the carriers used in marketed ASD products<sup>29</sup> as well as including polymers that are more novel for this purpose. Together, the polymers represent a wide range of functional moieties, hydrophilicity, glass transition temperatures and molecular weights, as shown in Table 2.

Table 2.

Selected polymeric carriers and their properties

Polymer	Supplier	$M_w$ [g mol <sup>-1</sup> ]	$T_g$ [°C]	Drug product examples*
HPMC 100LV <sup>a</sup>	DuPont	190,000	115	Sporanox®, Zortress®, Prograf®, Nivadil®
HPMCAS-M <sup>b,c</sup>	Shin-Etsu	55,000-93,000	122	Noxafil®, Incivek®, Kalydeco®, Symdeko®
CAP <sup>c</sup>	Sigma-Aldrich	N/A	160-170	N/A
PVP K25 <sup>d</sup>	BASF	28,000-34,000	165	Stivarga®, Cesamet®
PVP VA64 <sup>d</sup>	BASF	45,000-70,000	101	Rezulin®, Vosevi®, Eplclusa®, Lynparza®, Norvir®
Soluplus <sup>d</sup>	BASF	90,000-140,000	70	Febuxostat Zentiva®
Eudragit E <sup>e</sup>	Evonik	47,000	45	N/A
Eudragit L100 <sup>e</sup>	Evonik	125,000	>130	N/A

<sup>a</sup>DuPont product technical information, <sup>b</sup>Shin-Etsu product technical information, <sup>c</sup>Handbook of pharmaceutical excipients, 6th edition, Pharmaceutical press, <sup>d</sup>BASF product technical information, <sup>e</sup>Evonik product technical information. \*The ASD drug product examples are intended to be illustrative, not exhaustive. The examples do not necessarily contain the same polymer grade as used in this study. N/A: no information available.

## I. Differential scanning calorimetry

Differential scanning calorimetry (DSC) was used to evaluate the glass forming ability (GFA) of each of the APIs investigated in this study. Determination of melting points ( $T_m$ ) and glass transition temperatures ( $T_g$ ) was performed using a DSC 1 instrument (Mettler-Toledo AG, Greifensee, CH). The instrument was calibrated using an indium reference and nitrogen was used as purge gas with a flow rate of 150 mL min<sup>-1</sup>. All samples were prepared by weighing 2-4 mg of material into 40  $\mu$ L aluminum pans which were then hermetically sealed. Immediately before measurement, the sampling pan was pierced. The DSC heating cycle experiments were conducted using the approach designed by Baird *et al.*<sup>30</sup>. In brief, samples were heated at 10 °C min<sup>-1</sup> to approximately 10 °C above the melting temperature, held isothermally for 3 min, cooled at a rate of 20 °C min<sup>-1</sup> to -75 °C, and then reheated at 10 °C min<sup>-1</sup> to just above the melting temperature. From these DSC thermograms the  $T_m$  could be determined as the onset temperature of the melting endotherm during the first heat ramp and the  $T_g$  values were taken as the midpoint temperature of glass transition measured during the second heating ramp (*i.e.* after the sample was cooled at 20 °C min<sup>-1</sup>). Measurements were conducted on three samples in each case and reported as the average.

Based on these DSC cycles, the APIs could be classified according to their crystallization tendency in classes I-III. Class I compounds exhibit recrystallization during cooling from the undercooled melt state prior to the  $T_g$  event. Class II compounds recrystallize during reheating above  $T_g$  and class III do not crystallize upon either cooling to below  $T_g$  or upon subsequent reheating up to the melting point<sup>30</sup>.

## II. Small scale solubility determination in biorelevant medium

To determine the crystalline solubility of the investigated APIs, an excess of API, 10-15 mg per well, was dispensed volumetrically into a 96-well polypropylene plate (Microplate 96/F-PP, Eppendorf AG, Hamburg, DE) using a manual powder dispenser (Titan Resin Loader System, Spike International Ltd., Wilmington, NC). Parylene coated stirring bars and 200  $\mu$ L of FaSSiF-V1 medium were then added to the sample. The microtiter plates were then closed with pre-slit SepraSeal caps and equilibrated for 24 h at 37 °C in a conditioning cabinet by gentle head-over-head rotation using a Heidolph Reax 2 mixer (VWR International AG, Dietikon, CH) and a custom-built clamp device. After 24 h, 100  $\mu$ L of the API slurry was transferred to a 96-well filtration plate (MultiScreen® HTS, PCF, Merck Millipore Ltd, Cork, IRL) where filtration was carried out by centrifugation (Heraeus Omnisuge 2.0 RS, Kendro Laboratory Products AG, Zürich, CH). Determination of the API content in the filtrates was performed using UPLC. The pH of the remaining unfiltered slurry was measured to confirm that the pH had not changed by more than 0.05 units after 24 h. All experiments were performed in triplicate. As the solubility of itraconazole was below the limit of quantification for this method, a literature value was used for the solubility of this API<sup>31</sup>.

## III. Permeability prediction

The human effective permeability ( $P_{eff}$ ) of each API was predicted *in silico* using the ADMET Predictor version 10.4 (Simulations Plus Inc., Lancaster, CA, USA).

## IV. Solvent-based film casting of ASDs

A dissolution test was conducted using the same biorelevant medium and sample container as used for the solubility test. Binary amorphous films containing API and polymer were prepared by solvent film casting in 96-

well polypropylene microtiter plates (Microplate 96/F-PP, Eppendorf AG, Hamburg, DE) following the methodology of Wyttenbach *et al.*<sup>17</sup>. In brief, amorphous films containing befebutipitant, celecoxib or itraconazole were prepared respectively in combination with eight different polymers (Cellulose acetate phthalate, Eudragit E, Eudragit L100, HPMC 100LV, HPMCAS-M, PVP K25, PVP VA64 and Soluplus). Due to their varying solubility in organic solvent, solutions of API and polymer were prepared in either acetone, ethanol, methanol or a 1:1 solution of dichloromethane and ethanol or methanol at a concentration of 10 mg mL<sup>-1</sup>. These API and polymer solutions were mixed at appropriate ratios to achieve a final drug loading of 20, 30 and 40% [w/w] and transferred to individual wells of the microtiter plate. By transferring 50-100 µL of each mixture using Gilson M50 and M100 pipettes (Gilson, Mettmenstetten, CH), it was ensured that a consistent dose of 0.2 mg API was present in all wells. Two rows of the 96-well plate contained control samples, consisting of either 0.2 mg pure API or 1.8 mg pure polymer. The solvent was evaporated using heated nitrogen at 60 °C for 30 min using the Ultravap™ device (Zinsser Analytik GmbH, Frankfurt, DE). The solvent-cast films were stored overnight in a desiccator over silica blue gel at room temperature.

#### V. Miniaturized dissolution screening of solvent cast films for amorphous drug supersaturation maintenance

The dissolution screening of amorphous solvent-cast films was conducted in a similar manner as for the solubility studies. Here, a parylene coated stirring bar and 200 µL of FaSSIF-V1 medium was added to each well of the microtiter plates containing the amorphous films. Two plates were utilized to enable sampling at two different time points: one of the plates was sampled after 1 h and the other was sampled after 3 h. The plates were closed with pre-slit SeptraSeal caps and equilibrated at 37 °C by gentle head-over-head rotation. At the respective sampling points, 100 µL of the dissolution medium was transferred from the plate to a 96-well filtration plate (MultiScreen® HTS, PCF, Merck Millipore Ltd, Cork, IRL) where filtration was carried out by centrifugation (Heraeus Omnifuge 2.0 RS, Kendro Laboratory Products AG, Zürich, CH). All experiments were conducted in triplicate, with sampling at the 1 and 3 h time points. The filtrates were collected in 96-well polypropylene plate (Twin.tec skirted 96-well PCR plate, Eppendorf AG, Hamburg, DE) and immediately diluted appropriately with N-methyl-pyrrolidone (NMP). Determination of the API content in the filtrates was performed using UPLC and used to evaluate the extent of API supersaturation.

#### VI. Ultra performance liquid chromatography™

Quantification of API content was conducted using an Acquity Ultra Performance Liquid Chromatographic (UPLC)™ system coupled with a detector (2996 Photodiode Array Detector) and Waters Acquity UPLC™ BEH C18 (1.7 µm, 2.1 x 50 mm) column from Waters (Milford, MA, USA). The mobile phase consisted of phase A: 0.1% [v/v] formic acid in deionized water, and phase B: 0.1% [v/v] formic acid in acetonitrile. Here a gradient flow with a rate of 0.75 mL min<sup>-1</sup> was applied to achieve an analyte retention time of less than the run time of 1.2 min. The detection wavelengths of befebutipitant, celecoxib and itraconazole were 256, 220 and 223 nm respectively. The column temperature was kept constant at 30 °C and the sample injection volume was 2 µL.

#### VII. Standard investigations of the refined Developability Classification System

The rDCS standard investigations are used to evaluate the feasibility of developing an oral IR formulation for a given API, based on a dose classification in one of the five rDCS categories, depending on solubility and permeability of the API<sup>1, 2</sup>. In addition to classifying an API according to the solubility of the neat material, the

rDCS can also be used in early development to forecast shifts in classification and thus to project the benefit of various enabling formulations with respect to oral absorption. To do so, the dose-solubility ratio of the neat APIs was first calculated at projected doses, and then again for the APIs in their supersaturated state in combination with polymeric carriers. The following equations were applied<sup>3</sup>:

$$(1) D/S = \frac{Dose}{S_{small\ intestine}}$$

$$(2) D/S = \frac{Dose}{C_{super/formulation}}$$

where D/S is the dose-solubility ratio,  $S_{small\ intestine}$  is the equilibrium solubility of the API in a biorelevant medium simulating the environment of the small intestine and  $C_{super/formulation}$  is the estimated concentration reached in supersaturated solution (including possible excipient solubilizing effects).

### VIII. Data presentation

Graphical presentations were prepared using GraphPad Prism 10 (GraphPad Software Inc., La Jolla, CA, USA). All dissolution results presented for the selected APIs are expressed as mean values  $\pm$  standard deviation. Represented degrees of apparent supersaturation are calculated as the fold change. Molecular structures are represented in their skeletal structures and drawn using BIOVIA draw 2022 (Dassault systemès, Vélizy-Villacoublay, FR).

## Results and Discussion

### I. Differential scanning calorimetry

DSC was used to evaluate the GFA of each of the APIs investigated in this study. The melting points and glass transition temperatures of the APIs are reported in Table 1. The DSC thermograms revealed that the APIs befebutipant and itraconazole have superior GFAs. Since they do not recrystallize either during cooling from a melt or from reheating after cooling, they are classified as Class III glass formers according to the classification system of Baird *et al.*<sup>30</sup> This indicates a superior physical stability in the amorphous state with a low driving force for recrystallization and good compatibility with ASD formulation. One out of three celecoxib samples, however, exhibited recrystallization upon heating from a supercooled melt, resulting in a Class II classification indicating a lower physical stability in its vitrified state.

### II. Standard investigations of the refined Developability Classification System

The crystalline solubility of the selected APIs was measured in FaSSIF-V1 using a small-scale solubility setup and is presented in Table 2, along with the predicted human permeability.

Although the original rDCS paper argues that solubility data acquired from aspirated fasted state human intestinal fluids (FaHIF) are the “gold standard” for solubility data<sup>2</sup>, the accessibility and high costs of handling of the fluids has encouraged the use of biorelevant media to simulate the conditions of gastrointestinal tract<sup>32</sup>. A previously presented approach has been to predict FaHIF solubility from FaSSIF solubility data using a correlation of literature data. However, Beran *et al.* recently evaluated this approach and described that even with strict data inclusion criteria, the available literature FaHIF data is highly variable and cannot be used to make a confident prediction<sup>4</sup>. Therefore, such a correlation should be based on an in-house library of solubility values with consistent methodology to enhance predictability. If such a correlation is not available, it is recommended that FaSSIF solubility should be used for the classification as it has been shown to adequately reflect *in vivo* solubilities<sup>33</sup>.

The standard investigations of the rDCS, using FaSSIF-V1 solubilities, revealed that all three APIs would be classified as IIb at doses of 50 mg or more. This result indicates that the APIs are likely to exhibit solubility limited absorption. Furthermore, the rDCS also identifies the APIs as having high dose diversity risk levels of 3-4, further underlining that a considerable formulation effort is required to improve solubility and guarantee adequate absorption after oral administration<sup>2</sup>. Based on this outcome, the rDCS recommends initiation of an enabling formulation strategy. Since approaches like SPADS are specifically designed to rapidly screen a wide variety of ASD films, they are suitable for this purpose and can be used to streamline development.

Table 3.

Overview of rDCS classifications for investigated APIs

API	$P_{\text{eff}}$ [ $10^{-4}$ cm s <sup>-1</sup> ] <sup>a</sup>	FaSSIF-V1 solubility [ $\mu\text{g/mL}$ ]	rDCS class 5 mg dose	rDCS class 50 mg dose	rDCS class 500 mg dose	Risk level
Befetupitant	4.90	$9.1 \pm 0.3$	IIa	IIb	IIb	R3
Celecoxib	2.11	$41.3 \pm 1.8$	I	IIb	IIb	R3
Itraconazole	1.85	$0.3 \pm 0.0^{\text{b}}$	IIb	IIb	IIb	R4

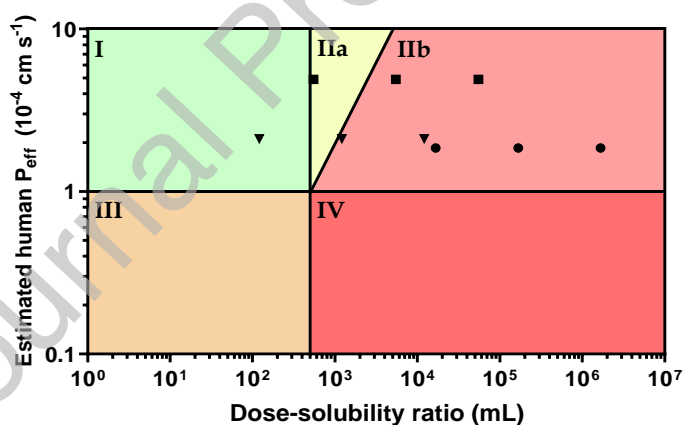
<sup>a</sup>Predicted value calculated using ADMET predictor version 10.4<sup>b</sup>Due to the measured value being <LOQ, a literature solubility value was used for the solubility of itraconazole in FaSSIF-V1<sup>31</sup>.

Figure 1. rDCS classification of befetupitant (■), celecoxib (▼) and itraconazole (●) at doses of 5, 50 and 500 mg.

### III. SPADS dissolution assay results

The APIs included in this study were chosen as they all exhibit satisfactory GFA and have sufficient solubility in volatile solvents, making them suitable candidates for solvent casting and ASD formulation. To evaluate the feasibility of ASD formulation for the selected APIs, a SPADS dissolution assay was conducted, using polymers with a wide range of functional moieties, to probe for preferential interaction between API and polymers in solution. The screening enables rapid rank ordering of the various ASD compositions and thereby quickly eliminate those that perform poorly. Using film-cast ASDs, the dissolution behavior of all three APIs was screened in binary combinations with the following carriers: HPMC 100LV, HPMCAS-M, CAP, PVP K25, PVP VA64,

Soluplus, Eudragit L100 and Eudragit E at drug loads of 20, 30 and 40 % using the SPADS dissolution assay with a nominal API concentration of 1 mg mL<sup>-1</sup>. A nominal API concentration of 1 mg mL<sup>-1</sup> corresponds to a 500 mg dose dissolved in 500 mL, which is the volume used to calculate the dose-solubility ratio in the rDCS. In addition to the binary combinations, reference samples containing neat solvent cast drug were analyzed to measure the kinetic solubility without the presence of polymer. The outcome of the GFA assessment showed that the investigated drugs do not have a high driving force for recrystallization upon vitrification and are expected to remain amorphous at the time of dissolution testing. Due to the nature of the SPADS dissolution assay, no solid-state investigations were performed for the ASD films however, if drug would revert to a crystalline form or generate amorphous-amorphous phase separation, this would be reflected in the achieved drug release. In the SPADS dissolution experiments the concentration of dissolved API was determined after 1 and 3 h incubation at 37 °C and the results are shown in Figure 2. The concentrations measured from these tests are reported in the Supplementary Materials (Tables S1 through S6). The results clearly show that the level of supersaturation is dependent on both the polymeric carrier used and the drug load applied, for all APIs.

### **Befetupitant**

Befetupitant, a discontinued Roche development compound, is a neurokinin-1 (NK1) receptor antagonist. This family of compounds are often used in the control of cancer chemotherapy-induced nausea and vomiting and in the treatment of mood disorders such as anxiety and depression<sup>34</sup>. As no marketed dose is available for befetupitant, the rDCS standard doses were used in the present study. The dissolution tests showed that four polymers showed especially promising dissolution results with respect to API release and stabilization of the supersaturated solution after three hours. The combination of Eudragit E and befetupitant showed the best performance at all investigated drug loads, reaching an apparent degree of supersaturation (aDS) of 82-92 at the three-hour time point. The performance of the cellulose derivatives was strongly dependent on the drug load, as shown in Figure 2, reaching relatively low aDS values of 8-27 at a 40 % drug load (DL), but values of 42-61 at 20 % DL. The results for cellulose derivatives indicate that a considerable amount of carrier is necessary to stabilize the supersaturated state. In previous studies, Eudragit E has been shown to interact with other APIs through hydrophobic interactions<sup>35</sup>, whereas the performance of the cellulose derivatives mostly depend on hydrogen bonding with the API and/or increased solution viscosity<sup>36</sup>.

### **Celecoxib**

Celecoxib is a nonsteroidal anti-inflammatory drug (NSAID) which is approved for multiple indications such as the treatment of osteo- and rheumatoid arthritis, ankylosing spondylitis, and acute pain<sup>37</sup>. In the case of Celecoxib, the ASD films tended to induce a lower but more consistent degree of supersaturation than for the other two APIs. Polymers which performed well include PVP VA64 and HPMCAS-M, which reached aDS values of 7 and 8, respectively, at the 40% drug load. The exception was Eudragit E, where good performance was demonstrated at the lowest drug load with an aDS of 12.5, but very poor performance was observed at drug loads of 30 and 40%. At higher drug loads, it appears that there is a lack of API release, as a concentration lower than the crystalline equilibrium solubility was measured. Similar behavior has previously been described, for which the term “limit of congruency” (LOC) was coined<sup>38, 39</sup>. LOC alludes to the fact that in some cases, increasing the drug load of an ASD may lead to unfavorable (in the current context) interactions between API and excipient, whereby neither will go fully into solution upon contact with an aqueous medium.

## Itraconazole

Itraconazole is a broad-spectrum systemic antifungal drug which inhibits ergosterol synthesis in the cell membrane of fungi<sup>40</sup>. For itraconazole, very clear differences in performance were observed across the polymers investigated. As can be seen in Figure 2, at a 20% drug load, ASD films containing either HPMC 100LV or Soluplus were able to reach full release at 1 h and maintained a degree of supersaturation of ~2900 and ~3100 fold respectively at the 3 h sampling time point. A lower but still considerable release was observed at the 30% DL for both ASD films. At a 40% DL the HPMC 100LV ASD films still shows a substantial effect by achieving an aDS of ~1500, underlining that this polymer is the consistently best performing carrier for itraconazole ASD films. At the 40% DL the API extent of supersaturation for the Soluplus ASD film was vastly decreased. These results align well with the fact that itraconazole has been marketed as an ASD using HPMC as the polymeric carrier (Sporanox®)<sup>41</sup>. However, the self-associating graft co-polymer Soluplus also shows great potential as a carrier and has also been reported to have a superior performance at a 40% [w/w] DL, based on a study of hot melt extruded tablets in beagle dogs<sup>42</sup>

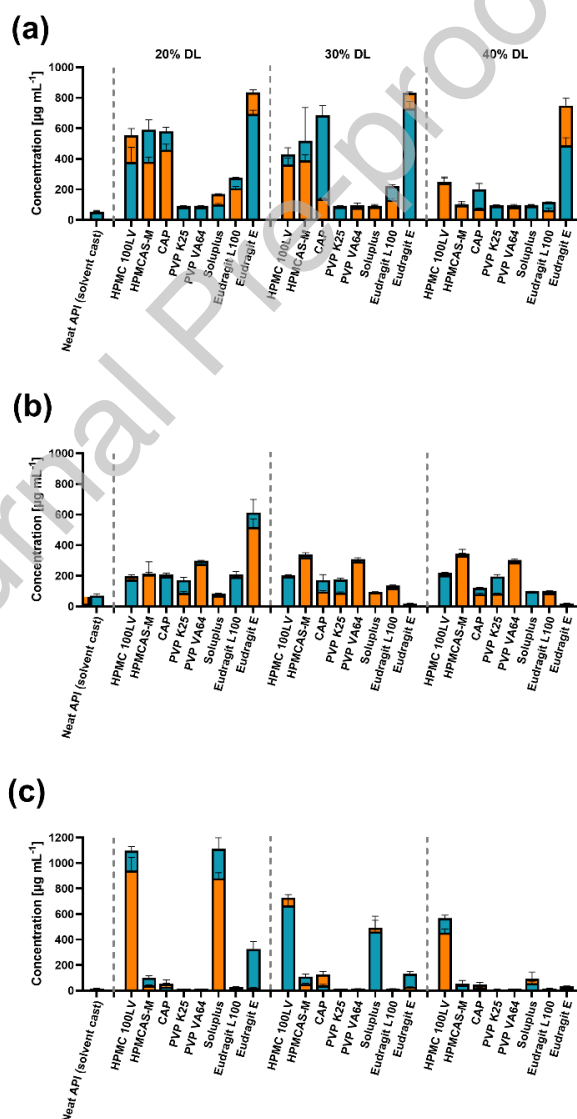


Figure 2. SPADS dissolution assay results for (a) befetupitant, (b) celecoxib and (c) itraconazole for all screened binary combinations, plotted as superimposed bars where blue represents 1 h data and orange represent 3 h data. DL: Drug Loading.

## IV. Implementation of SPADS dissolution assay results into the rDCS

Translating the dissolution results into the rDCS enables visualization of the change in rDCS classification resulting from ASD formulation compared to a conventional formulation containing the crystalline API.

**Befetupitant**

For befetupitant, vitrification of the API in the absence of a stabilizing excipient already causes a major shift in the rDCS class II space towards the cut-off between classes IIa and IIb (*i.e.* the solubility limited absorbable dose (SLAD)) represented by the diagonal line on the rDCS diagram. In the presence of an amorphous polymeric carrier, even higher concentrations of befetupitant were stabilized in solution, resulting in a further left-shift in the dose-solubility ratio.

At lower projected doses, such as the 50 mg dose, the left-shift in the rDCS classification was very apparent across all DLs. At the 40% DL, Eudragit E and HPMC 100LV enable stable supersaturation of befetupitant in amounts above the administered dose and the ASD would thereby move into rDCS class I (Figure 3.a). At this dose, a lower degree of supersaturation would be achieved as compared to the SPADS dissolution assay, in which a 10-fold higher dose was applied, so a decreased driving force for recrystallization is to be expected. All other polymers resulted in a classification change to rDCS class IIa, with a lower decrease in dose-solubility ratio.

For the “worst case” scenario, a dose of 500 mg, the combination of Eudragit E with befetupitant approaches the border between rDCS class I and IIa, indicating that almost the entire dose can be dissolved within three hours at the 40% DL (Figure 3.b). This result is significant, as the full dose would likely be dissolved and absorbed during transit through the intestine, given the compensatory relationship between solubility and permeability. At 500 mg, applying HPMC 100LV changed the rDCS classification to class IIa, albeit still close to the IIb border, whereas the other ASD films remained in class IIb with insufficient performance.

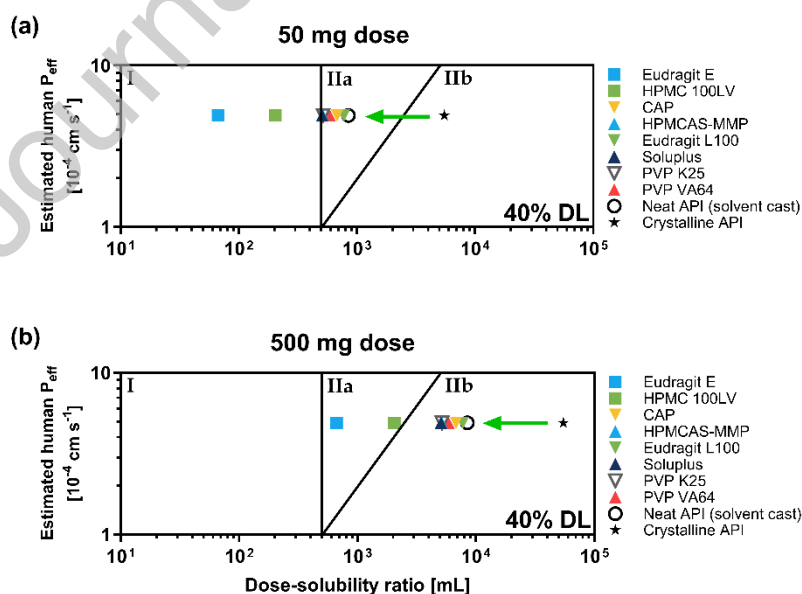


Figure 3. Compact rDCS plot showing the shift in befetupitant classification based on three-hour dissolution data at (a) 50 mg dose at 40% DL (b) 500 mg dose at 40% DL. The area representing class III and IV has been excluded out to simplify the plot, as no data points fell into these categories.

## Celecoxib

Overall, celecoxib gains a limited benefit from formulation as an ASD. Applying one of the marketed doses of celecoxib, 200 mg, the classification shift at the 20% DL crosses into the rDCS class I space for the Eudragit E ASD film (Figure 4.a). Similarly, a left-shift into rDCS class IIa is observed for PVP VA64 and the cellulose derivatives (HPMC 100LV, HPMCAS-M and CAP). Applying DLs of 30 or 40% did not result in any increase in performance beyond that of Eudragit E at 20% DL for any of the ASD films. However, it is noted that the use of a 20% DL formulation for a 200 mg dose may have limited appeal, as this would induce a high “pill burden” for the patient.

At the “worst case” dose of 500 mg dose all ASDs, except for the Eudragit E ASD film, remain in rDCS class IIb, although a small shift is observed within the class IIb space (Figure 4.b). The underwhelming dissolution performance of the ASD films along with the inferior GFA of celecoxib suggests that either a more suitable bioenabling formulation approach should be sought, or alternatively, the screening could be expanded to include ternary systems that may achieve a higher aDS.

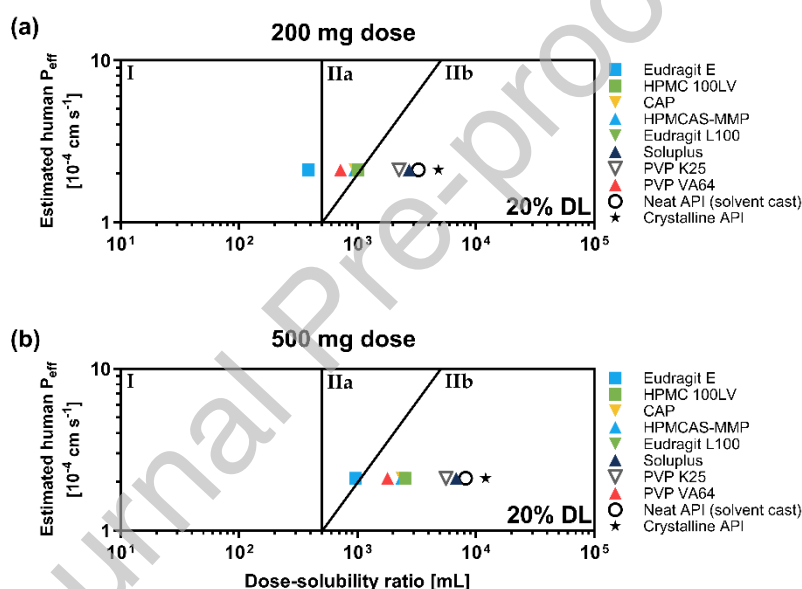


Figure 4. Compact rDCS plot showing the shift in celecoxib classification based on three-hour dissolution data at (a) 200 mg dose at 20% DL (b) 500 mg dose at 20% DL. The area representing class III and IV has been excluded out to simplify the plot, as no data points fell into these categories.

## Itraconazole

For itraconazole, translating the ASD dissolution results into the rDCS framework results in a significant left-shift from the neat crystalline API. Applying the marketed dose of itraconazole, 100 mg, demonstrates the impressive effect of HPMC 100LV as a carrier and precipitation inhibitor. For this formulation, the aDS is sufficient for the full dose to be released even at the 40% DL, as seen by the shift into class I, whereas all other screened ASD films remained in class IIb (Figure 5.a).

Applying the 40% DL results to the rDCS plots at the 500 mg dose, yields no classification change. At this dose the most apparent change is seen at the 20% DL where ASD films based on HPMC 100LV or Soluplus shift left to the border between rDCS class I and IIa (Figure 5.b).

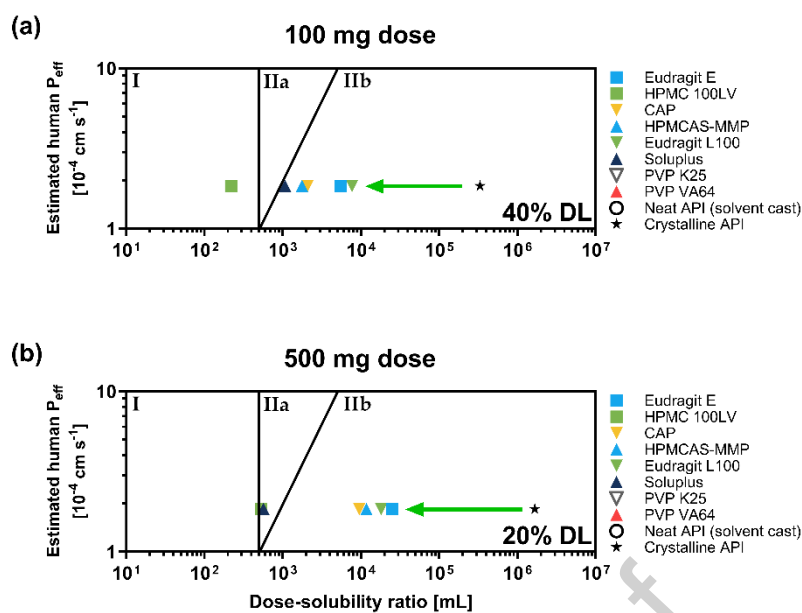


Figure 5. Compact rDCS plot showing the shift in itraconazole classification based on three-hour dissolution data at (a) 100 mg dose at 40% DL (b) 500 mg dose at 20% DL. The area representing class III and IV has been excluded out to simplify the plot, as no data points fell into these categories. Samples containing PVP K25, PVP VA64 and neat API (solvent cast) had concentrations below LOQ after three hours.

By calculating a dose-solubility ratio using the SPADS dissolution assay results for a projected dose lower than the actual screened dose, a prediction of the formulation's shift in the rDCS space can be made. When applying such doses, the achievable degree of supersaturation and driving force for recrystallization is adequately lowered, ensuring a reliable prediction of ASD performance. However, using a high dose during the dissolution tests may also lead to the exclusion of some polymeric carriers which may have had a sufficient effect at lower doses. Here it may be beneficial to perform confirmatory tests for carriers of special interest, in situations where the target dose is lower than 500 mg.

The dissolution method presented in this study relies on filtering the samples through a  $0.4 \mu\text{m}$  porous membrane. This experimental condition leads to the possibility that very fine particles or colloidal structures with a size of less than  $0.4 \mu\text{m}$  may pass through the filter membrane and be included in the final filtrate<sup>43, 44</sup>. These colloids are formed at concentrations above the amorphous solubility of an API and can give rise to an overprediction of the amount of API available for absorption and thereby the possible bioavailability advantage. Such colloidal species, *e.g.* liquid-liquid phase separated droplets, can also help to maintain a high concentration of freely dissolved API by acting as a reservoir and replenishing the bulk solution with API as it is absorbed<sup>43-46</sup>. However, by applying the three-hour dissolution data as the rDCS input, an overall estimate of the rDCS classification shift is achieved, as the true  $C_{max}$  and extent of supersaturation may not be fully captured by the sample at this time-point. Based on the outcome of the dissolution screening, compositions of interest can be prepared in a larger scale for further analysis. Methods of interest could be solvent shift testing to learn about the precipitation kinetics of the drug<sup>47, 48</sup>, or dissolution-permeation testing where an artificial membrane can be used to capture the interplay between supersaturation, precipitation and permeation of drug upon release<sup>49, 50</sup>.

The present study focused specifically on the use of ASDs as an enabling formulation strategy, but it should be noted that it is always advisable to identify a formulation strategy which is first and foremost compatible with the intrinsic properties of the API<sup>51-53</sup>. Many different options for enabling formulations exist, such as lipid-

based formulations, co-crystals or inclusion complex formation with *e.g.* cyclodextrins<sup>54</sup>. Analogous to SPADS, which is designed specifically for ASDs, the in vitro screening approaches for other types of enabling formulations can also be integrated into the rDCS to predict classification changes.

For discussions within project teams, the rDCS plot makes it possible to clearly identify specific candidate formulations that may allow for complete API release and bioavailability, which can then be selected for further development. After identifying the optimal API/carrier combination from the dissolution results, formulation development can proceed. The next step is to study the physical stability of the amorphous phase at increased temperature and humidity. This must be done to determine whether an adequate shelf-life for the product can be achieved. Concurrently, the homogeneity of the mixture should be investigated by *e.g.* atomic force microscopy<sup>55</sup> to reveal possible phase separation prior to scale up.

## Conclusion

This study has shown, for the first time, that by combining the SPADS dissolution assay as a screening tool with the rDCS, valuable information can be acquired and decision-making during formulation development can be shaped in a material-sparing, high throughput manner. Here, the rDCS was utilized first to classify each API and identify the need for solubility improvement. Based on the results, dissolution testing using solvent-cast films was carried out, and the release results fed back into the rDCS to predict the solubility benefit and guide selection of the polymeric carrier for the API. The SPADS/rDCS approach enables identification of the best performing ASD films. For the APIs studied, Eudragit E, HPMC 100LV and Soluplus showed especially advantageous effects as polymer carriers in multiple cases. This was further emphasized by the change in classification, where several ASD films were classified as rDCS class I, even though the rDCS classification of the API was initially class IIb. Based on the presented results, the approach could be expanded to include a diverse set of screening methods for enabling formulation strategies, where the rDCS can allow for a direct comparison and support formulation selection.

## Acknowledgements

This project has received funding from the European Union's Horizon 2020 research and innovation programme under the Marie Skłodowska-Curie grant agreement No. 955756. The data presented in this work was in part presented at the PBP world meeting in Vienna on 19<sup>th</sup> March 2024. The authors gratefully acknowledge Sara Bettonte (F. Hoffmann - La Roche Ltd.) for her support in predicting human  $P_{\text{eff}}$  values for the APIs investigated in this study.

## References

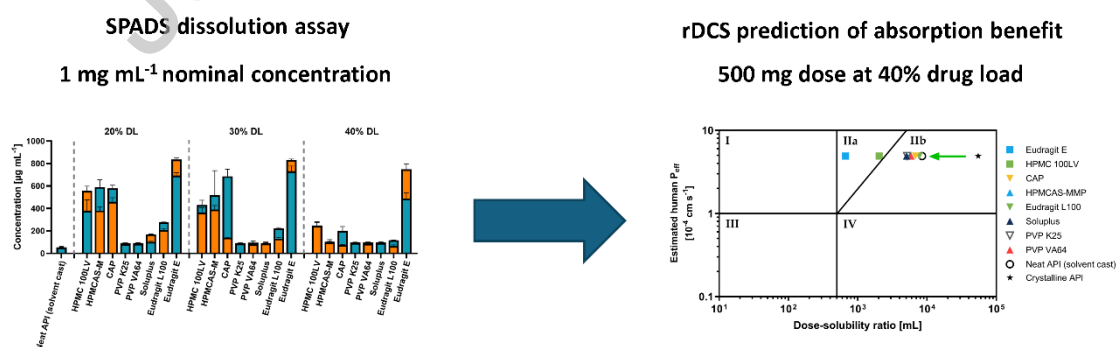
- (1) Butler J. M.; Dressman J. B. The developability classification system: application of biopharmaceutics concepts to formulation development. *J Pharm Sci.* 2010; 99 (12): 4940-4954.
- (2) Rosenberger J.; Butler J.; Dressman J. A Refined Developability Classification System. *J Pharm Sci.* 2018; 107 (8): 2020-2032.
- (3) Beran K.; Hermans E.; Holm R.; Sepassi K.; Dressman J. A Stratified Analysis of Supersaturation and Precipitation Effects Based on the Refined Developability Classification System (rDCS). *J Pharm Sci.* 2024; 113 (9): 2940-2946.
- (4) Beran K.; Hermans E.; Holm R.; Sepassi K.; Dressman J. Using the refined Developability Classification System (rDCS) to guide the design of oral formulations. *J Pharm Sci.* 2024; 113 (12): 3497-3517.

- (5) Babu N. J.; Nangia A. Solubility Advantage of Amorphous Drugs and Pharmaceutical Cocrystals. *Cryst Growth Des.* 2011; 11 (7): 2662-2679.
- (6) Van den Mooter G. The use of amorphous solid dispersions: A formulation strategy to overcome poor solubility and dissolution rate. *Drug Discov Today Technol.* 2012; 9 (2): e79-e85.
- (7) Brouwers J.; Brewster M. E.; Augustijns P. Supersaturating drug delivery systems: the answer to solubility-limited oral bioavailability? *J Pharm Sci.* 2009; 98 (8): 2549-2572.
- (8) Baghel S.; Cathcart H.; O'Reilly N. J. Polymeric Amorphous Solid Dispersions: A Review of Amorphization, Crystallization, Stabilization, Solid-State Characterization, and Aqueous Solubilization of Biopharmaceutical Classification System Class II Drugs. *J Pharm Sci.* 2016; 105 (9): 2527-2544.
- (9) Schittny A.; Huwyler J.; Puchkov M. Mechanisms of increased bioavailability through amorphous solid dispersions: a review. *Drug Deliv.* 2020; 27 (1): 110-127.
- (10) Bhujbal S. V.; Mitra B.; Jain U.; Gong Y.; Agrawal A.; Karki S.; et al. Pharmaceutical amorphous solid dispersion: A review of manufacturing strategies. *Acta Pharm Sin B.* 2021; 11 (8): 2505-2536.
- (11) Walden D. M.; Bunday Y.; Jagarapu A.; Antontsev V.; Chakravarty K.; Varshney J. Molecular Simulation and Statistical Learning Methods toward Predicting Drug-Polymer Amorphous Solid Dispersion Miscibility, Stability, and Formulation Design. *Molecules.* 2021; 26 (1): 182.
- (12) Walter S.; Mileo P. G. M.; Afzal M. A. F.; Kyeremateng S. O.; Degenhardt M.; Browning A. R.; et al. Predicting the Release Mechanism of Amorphous Solid Dispersions: A Combination of Thermodynamic Modeling and In Silico Molecular Simulation. *Pharmaceutics.* 2024; 16 (10): 1292.
- (13) Antolovic I.; Vrabec J.; Klajmon M. COSMOPharm: Drug-Polymer Compatibility of Pharmaceutical Amorphous Solid Dispersions from COSMO-SAC. *Mol Pharm.* 2024; 21 (9): 4395-4415.
- (14) Auch C.; Harms M.; Mader K. Melt-based screening method with improved predictability regarding polymer selection for amorphous solid dispersions. *Eur J Pharm Sci.* 2018; 124: 339-348.
- (15) Shadambikar G.; Kipping T.; Di-Gallo N.; Elia A. G.; Knuttel A. N.; Treffer D.; et al. Vacuum Compression Molding as a Screening Tool to Investigate Carrier Suitability for Hot-Melt Extrusion Formulations. *Pharmaceutics.* 2020; 12 (11): 1019.
- (16) Lauer M. E.; Maurer R.; Paepe A. T.; Stillhart C.; Jacob L.; James R.; et al. A Miniaturized Extruder to Prototype Amorphous Solid Dispersions: Selection of Plasticizers for Hot Melt Extrusion. *Pharmaceutics.* 2018; 10 (2): 58.
- (17) Wyttenbach N.; Janas C.; Siam M.; Lauer M. E.; Jacob L.; Scheubel E.; et al. Miniaturized screening of polymers for amorphous drug stabilization (SPADS): Rapid assessment of solid dispersion systems. *Eur J Pharm Biopharm.* 2013; 84 (3): 583-598.
- (18) Homayouni A.; Sadeghi F.; Nokhodchi A.; Varshosaz J.; Afrasiabi Garekani H. Preparation and characterization of celecoxib dispersions in soluplus(R): comparison of spray drying and conventional methods. *Iran J Pharm Res.* 2015; 14 (1): 35-50.
- (19) Fouad E. A.; El-Badry M.; Mahrous G. M.; Alanazi F. K.; Neau S. H.; Alsarra I. A. The use of spray-drying to enhance celecoxib solubility. *Drug Dev Ind Pharm.* 2011; 37 (12): 1463-1472.
- (20) Xie T.; Taylor L. S. Dissolution Performance of High Drug Loading Celecoxib Amorphous Solid Dispersions Formulated with Polymer Combinations. *Pharm Res.* 2016; 33 (3): 739-750.
- (21) Xie T.; Taylor L. S. Improved Release of Celecoxib from High Drug Loading Amorphous Solid Dispersions Formulated with Polyacrylic Acid and Cellulose Derivatives. *Mol Pharm.* 2016; 13 (3): 873-884.
- (22) Stewart A. M.; Grass M. E.; Brodeur T. J.; Goodwin A. K.; Morgen M. M.; Friesen D. T.; et al. Impact of Drug-Rich Colloids of Itraconazole and HPMCAS on Membrane Flux in Vitro and Oral Bioavailability in Rats. *Mol Pharm.* 2017; 14 (7): 2437-2449.
- (23) Davis M. T.; Potter C. B.; Mohammadpour M.; Albadarin A. B.; Walker G. M. Design of spray dried ternary solid dispersions comprising itraconazole, soluplus and HPMCP: Effect of constituent compositions. *Int J Pharm.* 2017; 519 (1-2): 365-372.
- (24) Bhardwaj V.; Trasi N. S.; Zemlyanov D. Y.; Taylor L. S. Surface area normalized dissolution to study differences in itraconazole-copovidone solid dispersions prepared by spray-drying and hot melt extrusion. *Int J Pharm.* 2018; 540 (1-2): 106-119.

- (25) Adhikari A.; Polli J. E. Characterization of Grades of HPMCAS Spray Dried Dispersions of Itraconazole Based on Supersaturation Kinetics and Molecular Interactions Impacting Formulation Performance. *Pharm Res.* 2020; 37 (10): 192.
- (26) Paulson S. K.; Vaughn M. B.; Jessen S. M.; Lawal Y.; Gresk C. J.; Yan B.; et al. Pharmacokinetics of celecoxib after oral administration in dogs and humans: effect of food and site of absorption. *J Pharmacol Exp Ther.* 2001; 297 (2): 638-645.
- (27) Heykants J.; Van Peer A.; Van de Velde V.; Van Rooy P.; Meuldermans W.; Lavrijsen K.; et al. The clinical pharmacokinetics of itraconazole: an overview. *Mycoses.* 1989; 32 Suppl 1: 67-87.
- (28) Tetko I. V.; Gasteiger J.; Todeschini R.; Mauri A.; Livingstone D.; Ertl P.; et al. Virtual computational chemistry laboratory--design and description. *J Comput Aided Mol Des.* 2005; 19 (6): 453-463.
- (29) Moseson D. E.; Tran T. B.; Karunakaran B.; Ambardekar R.; Hiew T. N. Trends in amorphous solid dispersion drug products approved by the U.S. Food and Drug Administration between 2012 and 2023. *Int J Pharm X.* 2024; 7: 100259.
- (30) Baird J. A.; Van Eerdenbrugh B.; Taylor L. S. A classification system to assess the crystallization tendency of organic molecules from undercooled melts. *J Pharm Sci.* 2010; 99 (9): 3787-3806.
- (31) Ozaki S.; Minamisono T.; Yamashita T.; Kato T.; Kushida I. Supersaturation-nucleation behavior of poorly soluble drugs and its impact on the oral absorption of drugs in thermodynamically high-energy forms. *J Pharm Sci.* 2012; 101 (1): 214-222.
- (32) Markopoulos C.; Andreas C. J.; Vertzoni M.; Dressman J.; Reppas C. In-vitro simulation of luminal conditions for evaluation of performance of oral drug products: Choosing the appropriate test media. *Eur J Pharm Biopharm.* 2015; 93: 173-182.
- (33) Dahlgren D.; Venczel M.; Ridoux J. P.; Skjold C.; Mullertz A.; Holm R.; et al. Fasted and fed state human duodenal fluids: Characterization, drug solubility, and comparison to simulated fluids and with human bioavailability. *Eur J Pharm Biopharm.* 2021; 163: 240-251.
- (34) Hoffmann T.; Bos M.; Stadler H.; Schnider P.; Hunkeler W.; Godel T.; et al. Design and synthesis of a novel, achiral class of highly potent and selective, orally active neurokinin-1 receptor antagonists. *Bioorg Med Chem Lett.* 2006; 16 (5): 1362-1365.
- (35) Saal W.; Ross A.; Wytenbach N.; Alsenz J.; Kuentz M. Unexpected Solubility Enhancement of Drug Bases in the Presence of a Dimethylaminoethyl Methacrylate Copolymer. *Mol Pharm.* 2018; 15 (1): 186-192.
- (36) Hong S.; Nowak S. A.; Wah C. L. Impact of Physicochemical Properties of Cellulosic Polymers on Supersaturation Maintenance in Aqueous Drug Solutions. *AAPS Pharm Sci Tech.* 2018; 19 (4): 1860-1868.
- (37) Gong L.; Thorn C. F.; Bertagnoli M. M.; Grosser T.; Altman R. B.; Klein T. E. Celecoxib pathways: pharmacokinetics and pharmacodynamics. *Pharmacogenet Genom.* 2012; 22 (4): 310-318.
- (38) Saboo S.; Kestur U. S.; Flaherty D. P.; Taylor L. S. Congruent Release of Drug and Polymer from Amorphous Solid Dispersions: Insights into the Role of Drug-Polymer Hydrogen Bonding, Surface Crystallization, and Glass Transition. *Mol Pharm.* 2020; 17 (4): 1261-1275.
- (39) Saboo S.; Mugheirbi N. A.; Zemlyanov D. Y.; Kestur U. S.; Taylor L. S. Congruent release of drug and polymer: A "sweet spot" in the dissolution of amorphous solid dispersions. *J Control Release.* 2019; 298: 68-82.
- (40) Hardin T. C.; Graybill J. R.; Fetchick R.; Woestenborghs R.; Rinaldi M. G.; Kuhn J. G. Pharmacokinetics of itraconazole following oral administration to normal volunteers. *Antimicrob Agents Chemother.* 1988; 32 (9): 1310-1313.
- (41) U.S. Food and Drug Administration, Sporanox® (Itraconazole) product label, [https://www.accessdata.fda.gov/drugsatfda\\_docs/label/2024/020083s0711bl.pdf](https://www.accessdata.fda.gov/drugsatfda_docs/label/2024/020083s0711bl.pdf), Reference ID: 5468184, Revised October 2024, Retrieved November 2024.
- (42) Zhong Y.; Jing G.; Tian B.; Huang H.; Zhang Y.; Gou J.; et al. Supersaturation induced by Itraconazole/Soluplus® micelles provided high GI absorption in vivo. *Asian J Pharm Sci.* 2016; 11 (2): 255-264.
- (43) Qian K.; Stella L.; Jones D. S.; Andrews G. P.; Du H.; Tian Y. Drug-Rich Phases Induced by Amorphous Solid Dispersion: Arbitrary or Intentional Goal in Oral Drug Delivery? *Pharmaceutics.* 2021; 13 (6): 889.
- (44) Nunes P. D.; Pinto J. F.; Henriques J.; Paiva A. M. Insights into the Release Mechanisms of ITZ:HPMCAS Amorphous Solid Dispersions: The Role of Drug-Rich Colloids. *Mol Pharmaceutics.* 2022; 19 (1): 51-66.

- (45) Indulkar A. S.; Gao Y.; Raina S. A.; Zhang G. G.; Taylor L. S. Exploiting the Phenomenon of Liquid-Liquid Phase Separation for Enhanced and Sustained Membrane Transport of a Poorly Water-Soluble Drug. *Mol Pharm.* 2016; *13* (6): 2059-2069.
- (46) Zhao P.; Han W.; Shu Y.; Li M.; Sun Y.; Sui X.; et al. Liquid-liquid phase separation drug aggregate: Merit for oral delivery of amorphous solid dispersions. *J Control Release.* 2023; *353*: 42-50.
- (47) Palmelund H.; Madsen C. M.; Plum J.; Mullertz A.; Rades T. Studying the Propensity of Compounds to Supersaturate: A Practical and Broadly Applicable Approach. *J Pharm Sci.* 2016; *105* (10): 3021-3029.
- (48) Plum J.; Madsen C. M.; Teleki A.; Bevernage J.; da Costa Mathews C.; Karlsson E. M.; et al. Investigation of the Intra- and Interlaboratory Reproducibility of a Small Scale Standardized Supersaturation and Precipitation Method. *Mol Pharm.* 2017; *14* (12): 4161-4169.
- (49) Lentz K. A.; Plum J.; Steffansen B.; Arvidsson P. O.; Omkvist D. H.; Pedersen A. J.; et al. Predicting in vivo performance of fenofibrate amorphous solid dispersions using in vitro non-sink dissolution and dissolution permeation setup. *Int J Pharm.* 2021; *610*: 121174.
- (50) Borbas E.; Kadar S.; Tsinman K.; Tsinman O.; Csicsak D.; Takacs-Novak K.; et al. Prediction of Bioequivalence and Food Effect Using Flux- and Solubility-Based Methods. *Mol Pharm.* 2019; *16* (10): 4121-4130.
- (51) Kuentz M.; Holm R.; Elder D. P. Methodology of oral formulation selection in the pharmaceutical industry. *Eur J Pharm Sci.* 2016; *87*: 136-163.
- (52) Singh A.; Worku Z. A.; Van den Mooter G. Oral formulation strategies to improve solubility of poorly water-soluble drugs. *Expert Opin Drug Del.* 2011; *8* (10): 1361-1378.
- (53) Reppas C.; Kuentz M.; Bauer-Brandl A.; Carlert S.; Dallmann A.; Dietrich S.; et al. Leveraging the use of in vitro and computational methods to support the development of enabling oral drug products: An InPharma commentary. *Eur J Pharm Sci.* 2023; *188*: 106505.
- (54) Buckley S. T.; Frank K. J.; Fricker G.; Brandl M. Biopharmaceutical classification of poorly soluble drugs with respect to "enabling formulations". *Eur J Pharm Sci.* 2013; *50* (1): 8-16.
- (55) Lauer M. E.; Siam M.; Tardio J.; Page S.; Kindt J. H.; Grassmann O. Rapid assessment of homogeneity and stability of amorphous solid dispersions by atomic force microscopy--from bench to batch. *Pharm Res.* 2013; *30* (8): 2010-2022.

### ASD developability screening of befetupitant



### Graphical abstract